Engineering Analysis with Boundary Elements 33 (2009) 778–788

Contents lists available at ScienceDirect

Engineering Analysis with Boundary Elements

journal homepage: www.elsevier.com/locate/enganabound

Numerical Green's functions for some electroelastic crack problems

L. Athanasius, W.T. Ang *, I. Sridhar

School of Mechanical and Aerospace Engineering, Nanyang Technological University, Republic of Singapore

ARTICLE INFO

Article history:
Received 7 October 2008
Accepted 15 January 2009
Available online 23 February 2009

Keywords:
Numerical Green's function
Boundary element method
Cracks
Piezoelectric solid

ABSTRACT

A plane electroelastic problem involving planar cracks in a piezoelectric body is considered. The deformation of the body is assumed to be independent of time and one of the Cartesian coordinates. The cracks are traction free and are electrically either permeable or impermeable. Numerical Green's functions which satisfy the boundary conditions on the cracks are derived using the hypersingular integral approach and applied to obtain a boundary integral solution for the electroelastic crack problem considered here. As the conditions on the cracks are built into the Green's functions, the boundary integral solution does not contain integrals over the cracks. It is used to derive a boundary element procedure for computing the crack tip stress and electrical displacement intensity factors.

1. Introduction

A well-established boundary element approach for solving crack problems is to use special Green's functions (modified fundamental solutions) chosen to satisfy the boundary conditions on the cracks. With an appropriate Green's function, the boundary integral formulation of the crack problem under consideration does not require integration over the crack faces. Consequently, difficulties associated with modeling the crack faces, such as singular stress at the crack tips and degenerate systems of linear algebraic equations, may be neatly avoided.

Such an approach for solving crack problems numerically was pioneered by Snyder and Cruse [22] when they derived an analytical Green's function for a single planar crack in an orthotropic elastic space of infinite extent. Subsequently, Clements and Haselgrove [10] extended the work in [22] to a general anisotropic elastic space, and Ang and Clements [4] further modified the Green's function to include the case of a fully closed planar crack. Special Green's functions for a planar crack and an arc crack in an isotropic elastic space were derived by Ang [2,3], respectively.

In general, it is difficult (if not impossible) to derive Green's functions analytically for cracks with arbitrary geometries, configurations and boundary conditions. To solve a wider range of crack problems, Telles et al. [23] proposed to derive the required Green's function numerically based on the hypersingular integral formulation of a suitable crack problem (see also [15]). (For some details on the hypersingular approach, one may refer to, for example, [8].) More recently, Ang and Telles [6] extended the numerical Green's function approach in [23] to solve an elastostatic problem involving multiple interacting planar cracks in an anisotropic body.

During the last 10 years or so, there has been considerable interest in the development of the boundary element method for fracture analysis of piezoelectric materials. Using Lekhnitskii's formalism and dislocation modeling, Rajapakse and Xu [20] obtained an analytical Green's function for a single traction free and electrically impermeable crack in a piezoelectric space. More recently, Garcia-Sanchez et al. [13] and Groh and Kuna [14] presented boundary element procedures based on boundary integral equations derived by using fundamental solution which does not satisfy the boundary conditions on the crack faces. In [14], opposite crack faces were modeled by using the so-called subdomain technique and quarter-point elements were employed to deal with the singular behaviors of the stress and electric displacement at the crack tips, while a dual (mixed) boundary integral formulation was used in [13] with the conditions on the cracks treated by a differentiated form of the usual boundary integral equations. Earlier works on boundary element methods for electroelastic crack problems include Xu and Rajapakse [25], Ding et al. [11] and Gao and Fan [12].

In the present paper, using the hypersingular integral approach, we derive numerical Green's functions for an arbitrary number of arbitrarily located planar cracks in an infinite piezoelectric space. The Green's functions are chosen to satisfy particular electroelastic boundary conditions on the cracks. Specifically, the boundary conditions are such that the cracks are traction free and electrically either permeable or impermeable. The analysis in Ang and Telles [6], based on the Stroh's formalism for anisotropic elasticity, serves as a useful guide here for the derivation of the numerical Green's functions, as

* Corresponding author.
E-mail address: mwtang@ntu.edu.sg (W.T. Ang).
URL: http://www.ntu.edu.sg/home/mwtang (W.T. Ang).

0955-7997/$ - see front matter © 2008 Elsevier Ltd. All rights reserved.
doi:10.1016/j.enganabound.2009.01.002

piezoelectric materials exhibit anisotropic behaviors when they deform. With the use of the special Green's functions, a boundary integral solution which does not require integration over the crack faces is obtained for a plane electroelastic problem involving planar cracks in a piezoelectric body. A simple boundary element procedure is outlined for the numerical solution of the crack problem. The displacement and electric potential jumps across opposite crack faces as well as the crack tip stress and electric displacement intensity factors may be readily and accurately computed once the elastic displacements, tractions, electric potential and electric displacement are all known on the boundary. To check the validity of the numerical Green's functions, the boundary element procedure is applied to solve some specific problems.

2. An electroelastic crack problem

With reference to a Cartesian co-ordinate frame denoted by $0x_1x_2x_3$, consider a homogeneous piezoelectric solid which contains M arbitrarily orientated planar cracks. The geometries of the solid and the cracks do not change along the x_3 direction. The interior of the solid is denoted by R, the exterior boundary by B and the k-th crack by $\gamma^{(k)}$. It is assumed that the cracks do not intersect with one another or the exterior boundary B. On the plane $x_3 = 0$, the boundary B appears as a simple closed curve and the crack $\gamma^{(k)}$ as a straight cut with tips $(a^{(k)}, b^{(k)})$ and $(c^{(k)}, d^{(k)})$. Refer to Fig. 1. For the purpose of the present paper, $\gamma^{(k)}$ is taken to be the directed straight line segment from $(a^{(k)}, b^{(k)})$ to $(c^{(k)}, d^{(k)})$.

At each and every point on the boundary B, either the displacements or the tractions and either the electric potential or the electric flux are prescribed. The prescribed conditions on B are independent of the spatial coordinate x_3 and time t and are such that the cracks become traction free. For the electrical conditions on the cracks, we consider separately two extreme cases: (a) electrically impermeable cracks and (b) electrically permeable cracks. Some discussions on electrically impermeable cracks versus permeable ones may be found in, for example, Shindo et al. [21] and Wang and Mai [24].

Mathematically, the boundary conditions on the cracks are given by

$$\sigma_{ij}(x_1,x_2)m_j^{(k)} \to 0 \quad \text{as } (x_1,x_2) \to (y_1,y_2) \in \gamma^{(k)} \text{ for } k = 1,2,\ldots,M, \tag{1}$$

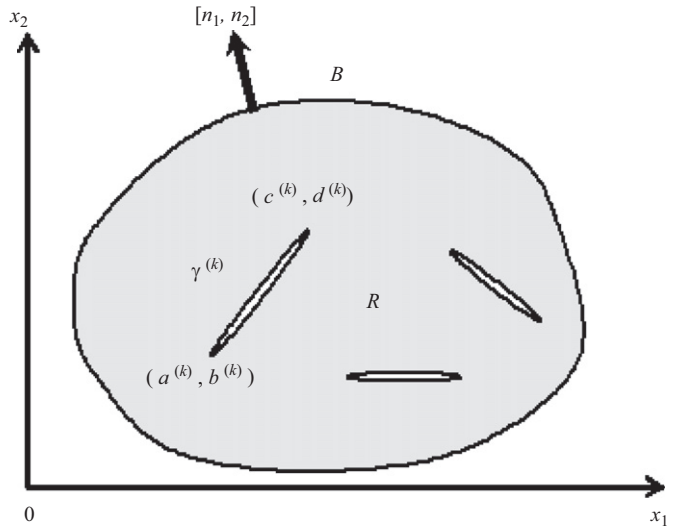

Fig. 1. A geometrical sketch of the problem.

and either

$$D_j(x_1,x_2)m_j^{(k)} \to 0 \quad \text{as } (x_1,x_2) \to (y_1,y_2) \in \gamma^{(k)} \text{ for } k = 1,2,\ldots,M$$
if the cracks are electrically impermeable, (2)

or

$$\Delta\phi(x_1,x_2) \to 0 \quad \text{and} \quad \Delta D(x_1,x_2) \to 0 \text{ as } (x_1,x_2) \to (y_1,y_2) \in \gamma^{(k)}$$
for $k = 1,2,\ldots,M$ if the cracks are electricallypermeable, (3)

where σ_{ij} and D_i are, respectively, the stresses and the electric displacements, $[m_1^{(k)}, m_2^{(k)}, m_3^{(k)}] = [(d^{(k)} - b^{(k)})/\ell^{(k)}, (a^{(k)} - c^{(k)})/\ell^{(k)}, 0]$ is a unit normal vector to the crack $\gamma^{(k)}$, $\ell^{(k)}$ is the length of $\gamma^{(k)}$ (that is, $\ell^{(k)} = \sqrt{(d^{(k)} - b^{(k)})^2 + (a^{(k)} - c^{(k)})^2}$) and $\Delta\phi$ is the jump in the electric potential ϕ across opposite crack faces as defined by

$$\Delta\phi(x_1,x_2) = \lim_{\varepsilon\to 0}[\phi(x_1 - |\varepsilon|m_1^{(k)}, x_2 - |\varepsilon|m_2^{(k)}) - \phi(x_1 + |\varepsilon|m_1^{(k)}, x_2 + |\varepsilon|m_2^{(k)})] \quad \text{for } (x_1,x_2) \in \gamma^{(k)}, \tag{4}$$

and ΔD is defined by

$$\Delta D(x_1,x_2) = \lim_{\varepsilon\to 0}[D_j(x_1 - |\varepsilon|m_1^{(k)}, x_2 - |\varepsilon|m_2^{(k)}) - D_j(x_1 + |\varepsilon|m_1^{(k)}, x_2 + |\varepsilon|m_2^{(k)})]m_j^{(k)} \quad \text{for } (x_1,x_2) \in \gamma^{(k)}. \tag{5}$$

To allow for antiplane deformations (that is, the case in which $u_3 \neq 0$), lowercase latin subscripts take the values of 1, 2 and 3. The usual Einsteinian convention of summing a repeated index is assumed for lowercase latin subscripts. In general, the summation over a repeated lowercase latin subscript (such as the subscript k in (6) and (7)) runs from 1 to 3. Nevertheless, for some cases, the summation may run from 1 to 2 only. For example, the summation over j in (1) and (2) is from 1 to 2 only as $m_3^{(k)} = 0$, and so is the summation over j and p in (6) and (7) since the displacements u_k are independent of x_3.

The problem is to determine the displacements u_k and the electric potential ϕ throughout the cracked piezoelectric solid.

3. Equations of electroelasticity

The governing equations for the displacements u_k and the electric potential ϕ in the piezoelectric solid are given by

$$c_{ijkp}\frac{\partial^2 u_k}{\partial x_j \partial x_p} + e_{pij}\frac{\partial^2 \phi}{\partial x_j \partial x_p} = 0,$$
$$e_{jkp}\frac{\partial^2 u_k}{\partial x_j \partial x_p} - \kappa_{jp}\frac{\partial^2 \phi}{\partial x_j \partial x_p} = 0, \tag{6}$$

where c_{ijkp}, e_{pij} and κ_{jp} are the constant elastic moduli, piezoelectric coefficients and dielectric coefficients, respectively.

The constitutive equations relating (σ_{ij}, D_j) and (u_k, ϕ) are given by

$$\sigma_{ij} = c_{ijkp}\frac{\partial u_k}{\partial x_p} + e_{pij}\frac{\partial \phi}{\partial x_p},$$
$$D_j = e_{jkp}\frac{\partial u_k}{\partial x_p} - \kappa_{jp}\frac{\partial \phi}{\partial x_p}. \tag{7}$$

Following closely the approach of Barnett and Lothe [7], we let

$$U_J = \begin{cases} u_j & \text{for } J = j = 1,2,3, \\ \phi & \text{for } J = 4, \end{cases}$$
$$S_{Ij} = \begin{cases} \sigma_{ij} & \text{for } I = i = 1,2,3, \\ D_j & \text{for } I = 4, \end{cases}$$

$$C_{IjKp}=\begin{cases} c_{ijkp} & \text{for } I=i=1,2,3 \text{ and } K=k=1,2,3,\\ e_{pij} & \text{for } I=i=1,2,3 \text{ and } K=4,\\ e_{jkp} & \text{for } I=4 \text{ and } K=k=1,2,3,\\ -\kappa_{jp} & \text{for } I=4 \text{ and } K=4, \end{cases} \tag{8}$$

so that (6) and (7) may be written more compactly as

$$C_{IjKp}\frac{\partial^2 U_K}{\partial x_j \partial x_p}=0 \tag{9}$$

and

$$S_{Ij}=C_{IjKp}\frac{\partial U_K}{\partial x_p}, \tag{10}$$

respectively. Note that uppercase latin subscripts have values 1–4. Summation is also implied for repeated uppercase latin subscripts running from 1 to 4.

The general solution of (9) can be written as

$$U_K(x_1,x_2)=\mathrm{Re}\left\{\sum_{\alpha=1}^{4}A_{K\alpha}f_\alpha(z_\alpha)\right\}, \tag{11}$$

where Re denotes the real part of a complex number, f_α are analytic functions of $z_\alpha=x_1+\tau_\alpha x_2$ in the domain of interest, τ_α are the solutions, with positive imaginary parts, of the 8-th order polynomial (characteristic) equation

$$\det[C_{I1K1}+(C_{I1K2}+C_{I2K1})\tau+C_{I2K2}\tau^2]=0 \tag{12}$$

and $A_{K\alpha}$ are solutions of the homogeneous system

$$[C_{I1K1}+(C_{I1K2}+C_{I2K1})\tau_\alpha+C_{I2K2}\tau_\alpha^2]A_{K\alpha}=0. \tag{13}$$

The characteristic equation (12) admits solutions which occur in complex conjugate pairs [7]. It is assumed that we can find τ_1, τ_2, τ_3 and τ_4 such that an invertible 4×4 matrix $[A_{K\alpha}]$ can be constructed from (13).

The generalized stress functions S_{Ij} corresponding to (11) are given by

$$S_{Ij}=\mathrm{Re}\left\{\sum_{\alpha=1}^{4}L_{Ij\alpha}f'_\alpha(z_\alpha)\right\}, \tag{14}$$

where the prime denotes differentiation with respect to the relevant argument and

$$L_{Ij\alpha}=(C_{IjK1}+\tau_\alpha C_{IjK2})A_{K\alpha}. \tag{15}$$

4. Numerical Green's functions

For the crack problem stated in Section 2, we seek to derive a function $\Phi_{KS}(x_1,x_2;\xi_1,\xi_2)$ satisfying the system of partial differential equations

$$C_{IjKp}\frac{\partial^2 \Phi_{KS}}{\partial x_j \partial x_p}=\delta_{IS}\delta(x_1-\xi_1,x_2-\xi_2), \tag{16}$$

and the conditions on the cracks given by either

$$\Psi_{IjS}(x_1,x_2;\xi_1,\xi_2)m_j^{(k)}\to 0 \quad \text{as } (x_1,x_2)\to(y_1,y_2)\in\gamma^{(k)}$$
$$\text{for } I=1,2,3,4 \text{ and } k=1,2,\ldots,M$$
$$\text{if the cracks are electrically impermeable} \tag{17}$$

or

$$\Psi_{IjS}(x_1,x_2;\xi_1,\xi_2)m_j^{(k)}\to 0, \quad \Delta\phi_{4S}(x_1,x_2;\xi_1,\xi_2)\to 0$$
$$\text{and } \Delta\Psi_S(x_1,x_2;\xi_1,\xi_2)\to 0 \quad \text{as } (x_1,x_2)\to(y_1,y_2)\in\gamma^{(k)}$$
$$\text{for } I=i=1,2,3 \text{ and } k=1,2,\ldots,M$$
$$\text{if the cracks are electrically permeable,} \tag{18}$$

where δ_{IS} is the Kronecker-delta, δ is the Dirac-delta function, Ψ_{IjS} and $\Delta\Psi_S$ are defined by

$$\Psi_{IjS}(x_1,x_2;\xi_1,\xi_2)=C_{IjRp}\frac{\partial \Phi_{RS}}{\partial x_p},$$
$$\Delta\Psi_S(x_1,x_2;\xi_1,\xi_2)=\lim_{\varepsilon\to 0}[\Psi_{4jS}(x_1-|\varepsilon|m_1^{(k)},x_2-|\varepsilon|m_2^{(k)};\xi_1,\xi_2)$$
$$-\Psi_{4jS}(x_1+|\varepsilon|m_1^{(k)},x_2+|\varepsilon|m_2^{(k)};\xi_1,\xi_2)]m_j^{(k)}$$
$$\text{for } (x_1,x_2)\in\gamma^{(k)}, \tag{19}$$

and $\Delta\phi_{4S}$ denotes the jump of Φ_{4S} across opposite crack faces as defined in (26).

Let $\Phi_{RS}(x_1,x_2;\xi_1,\xi_2)$ be given by

$$\Phi_{RS}(x_1,x_2;\xi_1,\xi_2)=\Phi_{RS}^{[1]}(x_1,x_2;\xi_1,\xi_2)+\Phi_{RS}^{[2]}(x_1,x_2;\xi_1,\xi_2), \tag{20}$$

$$\Phi_{RS}^{[1]}(x_1,x;\xi_1,\xi_2)=\frac{1}{2\pi}\mathrm{Re}\sum_{\alpha=1}^{4}\{A_{R\alpha}N_{\alpha J}\ln([x_1-\xi_1]+\tau_\alpha[x_2-\xi_2])\}\,d_{JS}, \tag{21}$$

where $[N_{\alpha J}]$ is the inverse of $[A_{K\alpha}]$, d_{JS} are real constants defined by

$$\mathrm{Im}\left\{\sum_{\alpha=1}^{4}L_{I2\alpha}N_{\alpha R}\right\}d_{RJ}=\delta_{IJ}. \tag{22}$$

Note that Im denotes the imaginary part of a complex number.

The function $\Phi_{RS}^{[1]}(x_1,x_2;\xi_1,\xi_2)$ in (21) is a solution of (16) (see, for example, [9]). It follows that $\Phi_{RS}^{[2]}(x_1,x_2;\xi_1,\xi_2)$ is required to satisfy

$$c_{IjKp}\frac{\partial^2 \Phi_{KS}^{[2]}}{\partial x_j \partial x_p}=0 \tag{23}$$

everywhere in the infinite piezoelectric space with the cracks $\gamma^{(1)}$, $\gamma^{(2)},\ldots,\gamma^{(M-1)}$ and $\gamma^{(M)}$.

Guided by the analysis in Ang and Park [5] and Ang and Telles [6], we take

$$\Phi_{RS}^{[2]}(x_1,x_2;\xi_1,\xi_2)=\sum_{k=1}^{M}\int_{\gamma^{(k)}}\Delta\phi_{PS}(y_1,y_2;\xi_1,\xi_2)$$
$$\times\Lambda_{PR}^{(k)}(x_1,x_2;y_1,y_2)\,ds(y_1,y_2), \tag{24}$$

where

$$\Lambda_{IS}^{(k)}(x_1,x_2;y_1,y_2)=-\frac{1}{2\pi}\mathrm{Re}\sum_{\alpha=1}^{4}\left\{\frac{T_{Ij\alpha S}m_j^{(k)}}{[x_1-y_1]+\tau_\alpha[x_2-y_2]}\right\},$$
$$T_{Ij\alpha S}=L_{Ij\alpha}N_{\alpha R}d_{RS}, \tag{25}$$

and

$$\Delta\phi_{PS}(x_1,x_2;\xi_1,\xi_2)=\lim_{\varepsilon\to 0}[\Phi_{PS}(x_1-|\varepsilon|m_1^{(k)},x_2-|\varepsilon|m_2^{(k)};\xi_1,\xi_2)$$
$$-\Phi_{PS}(x_1+|\varepsilon|m_1^{(k)},x_2+|\varepsilon|m_2^{(k)};\xi_1,\xi_2)]$$
$$\text{for } (x_1,x_2)\in\gamma^{(k)}. \tag{26}$$

Note that the integration over $\gamma^{(k)}$ in (24) is one over a directed straight line segment from $(a^{(k)},b^{(k)})$ to $(c^{(k)},d^{(k)})$. It is assumed that (ξ_1,ξ_2) does not lie on any of the cracks. The system in (23) is satisfied by (24).

4.1. Electrically impermeable cracks

Conditions (17) on the electrically impermeable cracks require that

$$C_{IjRp}\frac{\partial \Phi_{RS}^{[2]}}{\partial x_p}m_j^{(k)}\to\Lambda_{IS}^{(k)}(x_1,x_2,\xi_1,\xi_2)$$
$$\text{as } (x_1,x_2)\to(y_1,y_2)\in\gamma^{(k)} \text{ for } k=1,2,\ldots,M. \tag{27}$$

From (24), conditions (27) for electrically impermeable cracks give rise to the system of hypersingular integral equations

$$\mathscr{H}\int_{-1}^{1}\frac{\chi_{PK}^{(q)}\Delta\phi_{PS}^{(q)}(v,\xi_1,\xi_2)\,dv}{(t-v)^2}+\sum_{\substack{n=1\\n\neq q}}^{M}\int_{-1}^{1}\Delta\phi_{PS}^{(n)}(v,\xi_1,\xi_2)Y_{PK}^{(nq)}(v,t)\,dv$$
$$=\Lambda_{KS}^{(q)}(X_1^{(q)}(t),X_2^{(q)}(t),\xi_1,\xi_2)$$
$$\text{for } -1<t<1,\ K=1,2,3,4,\ S=1,2,3,4 \text{ and } q=1,2,\ldots,M, \tag{28}$$

where $\mathscr{H}$ indicates that the integral is to be interpreted in the Hadamard finite-part sense and

$$\Delta\phi_{PS}^{(n)}(v,\xi_1,\xi_2)=\Delta\phi_{PS}(X_1^{(n)}(v),X_2^{(n)}(v);\xi_1,\xi_2),$$
$$\chi_{PK}^{(q)}=\frac{1}{\pi}\mathrm{Re}\sum_{\alpha=1}^{4}\left\{\frac{\ell^{(q)}Q_{PKrj\alpha}m_r^{(q)}m_j^{(q)}}{[(c^{(q)}-a^{(q)})+\tau_\alpha(d^{(q)}-b^{(q)})]^2}\right\},$$
$$Y_{PK}^{(nq)}(v,t)=\frac{1}{4\pi}\mathrm{Re}\sum_{\alpha=1}^{4}\left\{\frac{\ell^{(n)}Q_{PKrj\alpha}m_r^{(q)}m_j^{(n)}}{[\Xi^{(nq)}(v,t)+\tau_\alpha\Theta^{(nq)}(v,t)]^2}\right\}, \tag{29}$$

where $Q_{PKrj\alpha}=(c_{Kr1}+\tau_\alpha c_{Kr2})T_{Pj\alpha I}$, $\Xi^{(nq)}(v,t)=X_1^{(n)}(v)-X_1^{(q)}(t)$, $\Theta^{(nq)}(v,t)=X_2^{(n)}(v)-X_2^{(q)}(t)$, $2X_1^{(n)}(t)=[c^{(n)}+a^{(n)}]+[c^{(n)}-a^{(n)}]t$ and $2X_2^{(n)}(t)=[d^{(n)}+b^{(n)}]+[d^{(n)}-b^{(n)}]t$.

The method in Kaya and Erdogan [17] is chosen to solve (28) numerically for $\Delta\phi_{PS}^{(n)}(v,\xi_1,\xi_2)$. Let $\Delta\Phi_{PS}^{(n)}(v,\xi_1,\xi_2)$ be given approximately by

$$\Delta\phi_{PS}^{(n)}(v,\xi_1,\xi_2)\simeq\sqrt{1-v^2}\sum_{j=1}^{J}\phi_{PS}^{(nj)}(\xi_1,\xi_2)U^{(j-1)}(v), \tag{30}$$

where $U^{(j)}(x)=\sin([j+1]\arccos(x))/\sin(\arccos(x))$ $(-1<x<1)$ is the j-th order Chebyshev polynomial of the second kind and $\phi_{PS}^{(nj)}(\xi_1,\xi_2)$ are parameters to be determined.

Through substituting (30) into (28) and collocating (28) by letting $t=t^{(i)}\equiv\cos([2i-1]\pi/[2J])$ for $i=1,2,\ldots,J$, a system of linear algebraic equations containing the unknowns $\phi_{PS}^{(ni)}(\xi_1,\xi_2)$ can be obtained as follows:

$$-\sum_{j=1}^{J}j\pi\phi_{PS}^{(qj)}(\xi_1,\xi_2)\chi_{PK}^{(q)}U^{(j-1)}(t^{(i)})$$
$$+\sum_{j=1}^{J}\sum_{\substack{n=1\\n\neq q}}^{M}\phi_{PS}^{(nj)}(\xi_1,\xi_2)\int_{-1}^{1}\sqrt{1-v^2}U^{(j-1)}(v)Y_{PK}^{(nq)}(v,t^{(i)})\,dv$$
$$=\Lambda_{KS}^{(q)}(X_1^{(q)}(t^{(i)}),X_2^{(q)}(t^{(i)}),\xi_1,\xi_2)$$
$$\text{for } i=1,2,\ldots,J,\ K=1,2,3,4,\ S=1,2,3,4 \text{ and } q=1,2,\ldots,M. \tag{31}$$

Once $\phi_{PS}^{(ni)}(\xi_1,\xi_2)$ are determined from (31), $\Phi_{RS}^{[2]}(x_1,x_2,\xi_1,\xi_2)$ can be calculated approximately using

$$\Phi_{RS}^{[2]}(x_1,x_2,\xi_1,\xi_2)\simeq\frac{1}{2}\sum_{n=1}^{M}\ell^{(n)}\sum_{j=1}^{J}\phi_{PS}^{(nj)}(\xi_1,\xi_2)\int_{-1}^{1}\sqrt{1-t^2}$$
$$\times U^{(j-1)}(t)\Lambda_{PR}^{(n)}(x_1,x_2,X_1^{(n)}(t),X_2^{(n)}(t))\,dt. \tag{32}$$

If the points (x_1,x_2) and (ξ_1,ξ_2) do not lie on any of the cracks, the numerical evaluation of $\Phi_{RS}^{[2]}(x_1,x_2,\xi_1,\xi_2)$ as given by (32) does not pose any mathematical difficulties. The definite integrals over the interval $[-1,1]$ in (31) and (32) can be easily and accurately computed by using the numerical quadrature formula (25.4.40) listed in Abramowitz and Stegun [1].

Note that in (31) the coefficient of the unknown $\phi_{PS}^{(qj)}(\xi_1,\xi_2)$ is independent of the uppercase latin subscript S and the point (ξ_1,ξ_2). Thus, in solving (31) to determine $\phi_{PS}^{(qj)}(\xi_1,\xi_2)$ for different values of the subscript S and for different points (ξ_1,ξ_2), the square matrix containing the coefficients of the unknowns has to be computed and processed only once. For example, if the LU decomposition technique together with backward substitutions is used to solve (31), we have to decompose the square matrix only once.

4.2. Electrically permeable cracks

Conditions (18) for electrically permeable cracks require the hypersingular integral equations (28) to be modified by taking $\Delta\phi_{4S}^{(n)}(v,\xi_1,\xi_2)=0$ and replacing $K=1,2,3,4$ with $K=k=1,2,3$. Consequently, if the cracks are electrically permeable, $\Phi_{RS}^{[2]}(x_1,x_2,\xi_1,\xi_2)$ can still be computed by using (32) but with $\phi_{4S}^{(nj)}(\xi_1,\xi_2)=0$. The remaining functions $\phi_{1S}^{(nj)}(\xi_1,\xi_2)$, $\phi_{2S}^{(nj)}(\xi_1,\xi_2)$ and $\phi_{3S}^{(nj)}(\xi_1,\xi_2)$ required by (32) for computing $\Phi_{RS}^{[2]}(x_1,x_2,\xi_1,\xi_2)$ are to be determined by solving (31) (with $\phi_{4S}^{(nj)}(\xi_1,\xi_2)=0$) for $K=k=1,2,3$ (instead of $K=1,2,3,4$).

5. A boundary element procedure

If Green's function $\Phi_{IK}(x_1,x_2,\xi_1,\xi_2)$ satisfying either (17) or (18) (depending on the electrical boundary conditions on the cracks), as given in Section 4 is used, a direct boundary integral formulation for the crack problem in Section 2 is given by

$$\lambda(\xi_1,\xi_2)U_K(\xi_1,\xi_2)=\int_B[U_I(x_1,x_2)\Gamma_{IK}(x_1,x_2;\xi_1,\xi_2)$$
$$-P_I(x_1,x_2)\Phi_{IK}(x_1,x_2,\xi_1;\xi_2)]\,ds(x_1,x_2), \tag{33}$$

where $\lambda(\xi_1,\xi_2)=1$ if (ξ_1,ξ_2) lies in the interior of R and $\lambda(\xi_1,\xi_2)=\frac{1}{2}$ if (ξ_1,ξ_2) lies on a smooth part of B, $P_I(x_1,x_2)=S_{Ij}(x_1,x_2)n_j(x_1,x_2)$, n_j are the components of the unit normal vector to the boundary B (as shown in Fig. 1) and

$$\Gamma_{IK}(x_1,x_2;\xi_1,\xi_2)=C_{IjRs}n_j(x_1,x_2)\frac{\partial}{\partial x_s}[\Phi_{RK}(x_1,x_2,\xi_1,\xi_2)].$$

Note that the path of integration in (33) is over only the exterior boundary B of the piezoelectric solid. To see how the boundary integral equations for system (9) may be derived, one may refer to Clements [9].

From the boundary conditions on the exterior boundary B, either $U_I=u_i$ or $P_I=p_i$ for $I=i=1,2,3$, and either $U_4=\phi$ or P_4 are known at each and every point on B. The boundary B and the integral equations in (33) can be discretized to determine approximately the unknown generalized displacements U_I and/or tractions P_I on B. To do this, the boundary B is approximated using N straight line segments denoted by $B^{(1)}$, $B^{(2)},\ldots,B^{(N-1)}$ and $B^{(N)}$. Across the segment $B^{(m)}$, the displacements U_I and the tractions P_I are approximated by constants $U_I^{(m)}$ and $P_I^{(m)}$, respectively. Through approximating (33), the unknown constants on the boundary elements $U_I^{(m)}$ and/or tractions $P_I^{(m)}$ can be determined from the system of linear algebraic equations:

$$\frac{1}{2}U_K^{(m)}=\sum_{n=1}^{N}U_I^{(n)}\int_{B^{(n)}}\Gamma_{IK}(x_1,x_2;\xi_1^{(m)},\xi_2^{(m)})\,ds(x_1,x_2)$$
$$-\sum_{n=1}^{N}P_I^{(n)}\int_{B^{(n)}}\Phi_{IK}(x_1,x_2;\xi_1^{(m)},\xi_2^{(m)})\,ds(x_1,x_2)$$
$$\text{for } m=1,2,\ldots,N, \tag{34}$$

where $(\xi_1^{(m)},\xi_2^{(m)})$ is the midpoint of $B^{(m)}$.

Once $U_I^{(m)}$ and $P_I^{(m)}$ are all determined, the generalized displacements U_K (and hence the stresses S_{Ij}) at any interior point (ξ_1,ξ_2) in R can be computed approximately using

$$U_K(\xi_1,\xi_2)=\sum_{n=1}^{N}U_I^{(n)}\int_{B^{(n)}}\Gamma_{IK}(x_1,x_2;\xi_1,\xi_2)\,ds(x_1,x_2)$$
$$-\sum_{n=1}^{N}P_I^{(n)}\int_{B^{(n)}}\Phi_{IK}(x_1,x_2;\xi_1,\xi_2)\,ds(x_1,x_2). \tag{35}$$

The crack displacement jumps $\Delta U_K(x_1,x_2)$ defined by

$$\Delta U_K(x_1,x_2) = \lim_{\varepsilon\to 0}[U_K(x_1-|\varepsilon|m_1^{(k)},x_2-|\varepsilon|m_2^{(k)}) - U_K(x_1+|\varepsilon|m_1^{(k)},x_2+|\varepsilon|m_2^{(k)})] \quad \text{for } (x_1,x_2)\in\gamma^{(k)} \tag{36}$$

can also be computed as explained below when $U_I^{(m)}$ and $P_I^{(m)}$ are all known.

5.1. Electrically impermeable cracks

If the cracks are electrically impermeable then $\Delta U_K(x_1,x_2)$ can be determined by solving the hypersingular integral equations (see [6]):

$$\mathscr{H}\int_{-1}^{1}\frac{\chi_{PK}^{(q)}\Delta U_P^{(q)}(v)\,dv}{(t-v)^2}+\sum_{\substack{n=1\\ n\neq q}}^{M}\int_{-1}^{1}\Delta U_P^{(n)}(v)Y_{PK}^{nq)}(v,t)\,dv = S_K^{(q)}(t)$$
$$\text{for } -1<t<1,\ K=1,2,3,4 \text{ and } q=1,2,\ldots,M, \tag{37}$$

where $\Delta U_P^{(q)}(v)$ $(-1<v<1)$ is a function that gives $\Delta U_P(x_1,x_2)$ at the point $(X_1^{(q)}(v),X_2^{(q)}(v))$ of the crack $\gamma^{(q)}$, and

$$S_K^{(q)}(t)=\sum_{n=1}^{N}C_{KjRs}m_j^{(q)} \times\int_{B^{(n)}}\left\{-U_I^{(n)}\frac{\partial}{\partial\xi_s}[I_{IR}^{[1]}(x_1,x_2;\xi_1,\xi_2)]\Big|_{(\xi_1,\xi_2)=(X_1^{(q)}(t),X_2^{(q)}(t))} +P_I^{(n)}\frac{\partial}{\partial\xi_s}[\Phi_{IR}^{[1]}(x_1,x_2,\xi_1;\xi_2)]\Big|_{(\xi_1,\xi_2)=(X_1^{(q)}(t),X_2^{(q)}(t))}\right\}ds(x_1,x_2). \tag{38}$$

Note that (37) is derived using the boundary conditions in (1) and (2) and $S_K^{(q)}(t)$ is regarded as known after (34) is solved.

The system in (37) can be solved numerically using the same method for (28). The unknown functions $\Delta U_P^{(n)}(v)$ are approximated using

$$\Delta U_P^{(n)}(v)\simeq\sqrt{1-v^2}\sum_{j=1}^{J}\psi_P^{(nj)}U^{(j-1)}(v), \tag{39}$$

where $\psi_P^{(nj)}$are constants determined by the system of linear algebraic equations

$$-\sum_{j=1}^{J}j\pi\psi_P^{(qj)}\chi_{PK}^{(q)}U^{(j-1)}(t^{(i)}) +\sum_{j=1}^{J}\sum_{\substack{n=1\\ n\neq q}}^{M}\psi_P^{(nj)}\int_{-1}^{1}\sqrt{1-v^2}U^{(j-1)}(v)Y_{PK}^{nq)}(v,t^{(i)})\,dv = S_K^{(q)}(t^{(i)}) \quad \text{for } i=1,2,\ldots,J, K=1,2,3,4 \text{ and } q=1,2,\ldots,M, \tag{40}$$

where $t^{(i)}=\cos([2i-1]\pi/[2J])$ as in (31).

Note that the unknown $\psi_p^{(qj)}$ in (40) has the same coefficient as $\phi_{PS}^{(qj)}(\xi_1,\xi_2)$ in (31). Thus, in solving (40) for the unknowns $\psi_P^{(qj)}$, it is not necessary to set up and process again the matrix containing the coefficients of the unknowns.

Once the unknowns $\psi_P^{(qj)}$ are determined, $\Delta U_K(x_1,x_2)$ can be approximately computed using (39) and crack parameters of practical interest, such as the stress and electric displacement intensity factors, can also be extracted.

5.2. Electrically permeable cracks

If the cracks are electrically permeable then (37) has to be modified by setting $\Delta U_4^{(n)}(v)=0$ and replacing $K=1,2,3,4$ by $K=k=1,2,3$. It follows that we can solve (40), with $\psi_4^{(qj)}=0$ and $K=k=1,2,3$, for $\psi_1^{(qj)}$, $\psi_2^{(qj)}$ and $\psi_3^{(qj)}$ in order to determine $\Delta U_1^{(n)}(v)$, $\Delta U_2^{(n)}(v)$ and $\Delta U_3^{(n)}(v)$.

6. Specific problems

In this section, the boundary element procedure together with the numerical Green's functions above is applied to solve some specific problems involving a particular piezoelectric material. The piezoelectric material is such that it becomes elastically transversely isotropic under the action of the electric field, with the transverse plane being perpendicular to the electrical poling direction. The electroelastic properties of such a material are characterized by 10 independent constants denoted here by A, N, F, C, L, e_1, e_2, e_3, ε_1 and ε_2.

Problem 1. The exterior boundary of the solution domain R (on the plane $x_3=0$) is taken to be the sides of a square with vertices (h,h), $(-h,h)$, $(-h,-h)$ and $(h,-h)$. The interior of R contains a single electrically *impermeable* crack which occupies the region $-a<x_1<a$, $x_2=0$, where h and a are positive constants such that $a<h$. Here we take the crack tips to be $(a^{(1)},b^{(1)})=(-a,0)$ and $(c^{(1)},d^{(1)})=(a,0)$.

The electrical poling direction is taken to be along the x_2 direction with the constitutive equations given by

$$\begin{pmatrix}\sigma_{11}\\ \sigma_{22}\\ \sigma_{33}\\ \sigma_{32}\\ \sigma_{31}\\ \sigma_{12}\end{pmatrix}=\begin{pmatrix}A & F & N & 0 & 0 & 0\\ F & C & F & 0 & 0 & 0\\ N & F & A & 0 & 0 & 0\\ 0 & 0 & 0 & L & 0 & 0\\ 0 & 0 & 0 & 0 & \frac{1}{2}(A-N) & 0\\ 0 & 0 & 0 & 0 & 0 & L\end{pmatrix}\begin{pmatrix}\gamma_{11}\\ \gamma_{22}\\ \gamma_{33}\\ 2\gamma_{32}\\ 2\gamma_{31}\\ 2\gamma_{12}\end{pmatrix} -\begin{pmatrix}0 & e_2 & 0\\ 0 & e_3 & 0\\ 0 & e_2 & 0\\ 0 & 0 & e_1\\ 0 & 0 & 0\\ e_1 & 0 & 0\end{pmatrix}\begin{pmatrix}E_1\\ E_2\\ E_3\end{pmatrix} \tag{41}$$

and

$$\begin{pmatrix}D_1\\ D_2\\ D_3\end{pmatrix}=\begin{pmatrix}0 & 0 & 0 & 0 & 0 & e_1\\ e_2 & e_3 & e_2 & 0 & 0 & 0\\ 0 & 0 & 0 & e_1 & 0 & 0\end{pmatrix}\begin{pmatrix}\gamma_{11}\\ \gamma_{22}\\ \gamma_{33}\\ 2\gamma_{32}\\ 2\gamma_{31}\\ 2\gamma_{12}\end{pmatrix} +\begin{pmatrix}\varepsilon_1 & 0 & 0\\ 0 & \varepsilon_2 & 0\\ 0 & 0 & \varepsilon_1\end{pmatrix}\begin{pmatrix}E_1\\ E_2\\ E_3\end{pmatrix}, \tag{42}$$

where $2\gamma_{kj}=\partial u_k/\partial x_j+\partial u_j/\partial x_k$ and $E_k=-\partial\phi/\partial x_k$. Note that $\gamma_{33}=0$ and $E_3=0$ here since u_k and ϕ are independent of x_3.

From (6)–(8), (41) and (42), the non-zero coefficients C_{ijKp} are

$$
\begin{aligned}
&C_{1111}=C_{3333}=A,\quad C_{1133}=C_{3311}=N,\quad C_{2222}=C,\\
&C_{1122}=C_{2211}=C_{2233}=C_{3322}=F,\\
&C_{1212}=C_{2112}=C_{2121}=C_{1221}=C_{2323}=C_{3223}=C_{3232}=C_{2332}=L,\\
&C_{1313}=C_{3113}=C_{3131}=C_{1331}=\tfrac{1}{2}(A-N),\\
&C_{2141}=C_{1241}=C_{3243}=C_{2343}=C_{4121}=C_{4112}=C_{4332}=C_{4323}=e_1,\\
&C_{1142}=C_{3342}=C_{4211}=C_{4233}=e_2,\\
&C_{2242}=C_{4222}=e_3,\quad C_{4141}=C_{4343}=-\varepsilon_1,\quad C_{4242}=-\varepsilon_2.
\end{aligned}
\tag{43}
$$

According to (13), the matrix $[A_{K\alpha}]$ can then be obtained by finding non-trivial solutions of the homogeneous systems

$$
\begin{pmatrix}
A+L\tau_\alpha^2 & (F+L)\tau_\alpha & 0 & (e_1+e_2)\tau_\alpha\\
(F+L)\tau_\alpha & L+C\tau_\alpha^2 & 0 & e_1+e_3\tau_\alpha^2\\
0 & 0 & \frac{1}{2}(A-N)+L\tau_\alpha^2 & 0\\
(e_1+e_2)\tau_\alpha & e_1+e_3\tau_\alpha^2 & 0 & -\varepsilon_1-\varepsilon_2\tau_\alpha^2
\end{pmatrix}
\begin{pmatrix}A_{1\alpha}\\A_{2\alpha}\\A_{3\alpha}\\A_{4\alpha}\end{pmatrix}
=\begin{pmatrix}0\\0\\0\\0\end{pmatrix},
\tag{44}
$$

where

$$
\tau_3=i\sqrt{\frac{A-N}{2L}}\quad (A>N),
\tag{45}
$$

and τ_1, τ_2 and τ_4 are solutions (with positive imaginary parts) of the sextic equation in τ given by

$$
\det\begin{pmatrix}
A+L\tau^2 & (F+L)\tau & (e_1+e_2)\tau\\
(F+L)\tau & L+C\tau^2 & e_1+e_3\tau^2\\
(e_1+e_2)\tau & e_1+e_3\tau^2 & -\varepsilon_1-\varepsilon_2\tau^2
\end{pmatrix}=0.
\tag{46}
$$

For $\alpha=3$, a non-trivial solution of (44) which forms the third column of the matrix $[A_{K\alpha}]$ is given by

$$
\begin{pmatrix}A_{13}\\A_{23}\\A_{33}\\A_{43}\end{pmatrix}=\begin{pmatrix}0\\0\\1\\0\end{pmatrix}.
\tag{47}
$$

For $\alpha=1$, 2 and 4, if $(A+L\tau_\alpha^2)(L+C\tau_\alpha^2)-(F+L)^2\tau_\alpha^2\neq 0$, we may take $A_{3\alpha}=0$ and $A_{4\alpha}=1$ and find $A_{1\alpha}$ and $A_{2\alpha}$ by solving

$$
\begin{pmatrix}A+L\tau_\alpha^2 & (F+L)\tau_\alpha\\(F+L)\tau_\alpha & L+C\tau_\alpha^2\end{pmatrix}\begin{pmatrix}A_{1\alpha}\\A_{2\alpha}\end{pmatrix}=-\begin{pmatrix}(e_1+e_2)\tau_\alpha\\e_1+e_3\tau_\alpha^2\end{pmatrix},
\tag{48}
$$

in order to construct the first, second and fourth columns of the matrix $[A_{K\alpha}]$.

For the crack in the region $-a<x_1<a$, $x_2=0$, we define the crack tip stress intensity factors $K_{\mathrm{I}}^{\pm}$, $K_{\mathrm{II}}^{\pm}$ and $K_{\mathrm{III}}^{\pm}$ and electric displacement intensity factors $K_{\mathrm{IV}}^{\pm}$ by

$$
\begin{aligned}
&K_{\mathrm{I}}^{+}=\lim_{x\to a^+}\sqrt{2(x-a)}S_{22}(x,0),\quad K_{\mathrm{I}}^{-}=\lim_{x\to -a^-}\sqrt{-2(x+a)}S_{22}(x,0),\\
&K_{\mathrm{II}}^{+}=\lim_{x\to a^+}\sqrt{2(x-a)}S_{12}(x,0),\quad K_{\mathrm{II}}^{-}=\lim_{x\to -a^-}\sqrt{-2(x+a)}S_{12}(x,0),\\
&K_{\mathrm{III}}^{+}=\lim_{x\to a^+}\sqrt{2(x-a)}S_{32}(x,0),\quad K_{\mathrm{III}}^{-}=\lim_{x\to -a^-}\sqrt{-2(x+a)}S_{32}(x,0),\\
&K_{\mathrm{IV}}^{+}=\lim_{x\to a^+}\sqrt{2(x-a)}S_{42}(x,0),\quad K_{\mathrm{IV}}^{-}=\lim_{x\to -a^-}\sqrt{-2(x+a)}S_{42}(x,0).
\end{aligned}
\tag{49}
$$

If $\Delta U_P^{(1)}(v)$ are approximately given by (39) (with $n=1$) then we can compute $K_{\mathrm{I}}^{\pm}$, $K_{\mathrm{II}}^{\pm}$, $K_{\mathrm{III}}^{\pm}$ and $K_{\mathrm{IV}}^{\pm}$ numerically using

$$
\begin{aligned}
K_{\mathrm{I}}^{\pm}&\simeq \mathrm{sgn}(-m_2^{(1)})\frac{w_{P2}}{\sqrt{a}}\sum_{j=1}^{J}\psi_P^{(1j)}U^{(j-1)}(\pm 1),\\
K_{\mathrm{II}}^{\pm}&\simeq \mathrm{sgn}(-m_2^{(1)})\frac{w_{P1}}{\sqrt{a}}\sum_{j=1}^{J}\psi_P^{(1j)}U^{(j-1)}(\pm 1),\\
K_{\mathrm{III}}^{\pm}&\simeq \mathrm{sgn}(-m_2^{(1)})\frac{w_{P3}}{\sqrt{a}}\sum_{j=1}^{J}\psi_P^{(1j)}U^{(j-1)}(\pm 1),\\
K_{\mathrm{IV}}^{\pm}&\simeq \mathrm{sgn}(-m_2^{(1)})\frac{w_{P4}}{\sqrt{a}}\sum_{j=1}^{J}\psi_P^{(1j)}U^{(j-1)}(\pm 1),
\end{aligned}
\tag{50}
$$

where $w_{PK}=-\mathrm{Re}\{(Q_{PK221}+Q_{PK222}+Q_{PK223}+Q_{PK224})/2\}$ and $\mathrm{sgn}(x)$ denotes the sign of x (that is, it is given by -1 and 1 for $x<0$ and $x>0$, respectively).

A particular solution U_K satisfying (9) in the whole of the $0x_1x_2$ plane with a cut in the region $-a<x_1<a$, $x_2=0$ and the corresponding S_{Kj} are given by

$$
\begin{aligned}
U_K&=\mathrm{Re}\left\{\sum_{\alpha=1}^{4}A_{K\alpha}(M_{\alpha 2}+M_{\alpha 4})(z_\alpha^2-a^2)^{1/2}\right\},\\
S_{Kj}&=\mathrm{Re}\left\{\sum_{\alpha=1}^{4}L_{Kj\alpha}(M_{\alpha 2}+M_{\alpha 4})\frac{z_\alpha}{(z_\alpha^2-a^2)^{1/2}}\right\},
\end{aligned}
\tag{51}
$$

where $z_\alpha=x_1+\tau_\alpha x_2$ and $[M_{\alpha S}]$ is the inverse matrix of $[L_{K2\alpha}]$. It may be verified that with (51) the conditions that the crack $-a<x_1<a$, $x_2=0$ is traction-free and electrically impermeable are satisfied, that is, $S_{K2}=0$ (for $K=1$, 2, 3 and 4) on the crack. Note that the branch for $(z_\alpha^2-a^2)^{1/2}$ in (51) is chosen such that

$$
\lim_{|z_\alpha|\to\infty}\frac{(z_\alpha^2-a^2)^{1/2}}{z_\alpha}=1.
\tag{52}
$$

For a particular test problem involving the electrically impermeable crack, (51) is used to generate boundary values of U_K and P_K on the horizontal and vertical sides of the square domain R, respectively. For mere illustrative purposes, we use the material constants of a class of PZT4 piezoceramics in our calculation, that is,

$$
\begin{aligned}
&A=13.9\times 10^{10},\quad N=7.78\times 10^{10},\quad F=7.43\times 10^{10},\\
&C=11.3\times 10^{10},\quad L=2.56\times 10^{10},\\
&e_1=13.44,\quad e_2=-6.98,\quad e_3=13.84,\\
&\varepsilon_1=60\times 10^{-10},\quad \varepsilon_2=54.7\times 10^{-10}.
\end{aligned}
\tag{53}
$$

The values of A, N, F, C and L above are in $\mathrm{N/m^2}$, e_1, e_2 and e_3 are in $\mathrm{C/m^2}$, and ε_1 and ε_2 are in $\mathrm{C/(V\,m)}$. These values are taken from Park and Sun [19].

Each side of the square region $-h<x_1<h$, $-h<x_2<h$ is discretized into N_0 equal length elements, so that the total number of elements is $4N_0$. For $a=1$ and $h=2$, two sets of numerical calculations are carried out using the boundary element method. Set A is obtained by using $N_0=10$ (40 elements), while Set B by $N_0=40$ (160 elements). The numerical Green's function for the impermeable crack is calculated using $J=10$ in (32).

Numerical values of the elastic displacement ($U_1\times 10^{12}$, $U_2\times 10^{12}$) and the electric potential $U_4\times 10^3$ at selected points in the interior of the square domain are compared with the exact values computed using (51) in Tables 1 and 2, respectively. (Note that $U_3=0$ for the particular problem here.) Both sets of numerical values for U_1, U_2 and U_4 are reasonably close to the exact ones. On the whole, the numerical values in Set B are more accurate than

Table 1
Numerical and exact values of $(U_1 \times 10^{12}, U_2 \times 10^{12})$ at selected interior points.

Point (x_1, x_2)	Set A $(U_1, U_2) \times 10^{12}$	Set B $(U_1, U_2) \times 10^{12}$	Exact $(U_1, U_2) \times 10^{12}$
(1.10, 0.00)	(2.5808, 0.0000)	(2.6165, 0.0000)	(2.6297, 0.0000)
(0.50, 0.80)	(4.9294, 15.936)	(4.9304, 15.840)	(4.9312, 15.807)
(0.10, 0.70)	(1.0309, 17.915)	(1.0311, 17.815)	(1.0312, 17.780)
(1.90, 0.10)	(9.2099, 0.82173)	(9.3035, 0.74540)	(9.3331, 0.74065)
(0.90, 0.20)	(5.8260, 8.8090)	(5.8412, 8.7584)	(5.8655, 8.7773)
(1.05, 1.05)	(8.4852, 12.839)	(8.4864, 12.746)	(8.4887, 12.716)

Table 2
Numerical and exact values of $U_4 \times 10^3$ at selected interior points.

Point (x_1, x_2)	Set A $U_4 \times 10^3$	Set B $U_4 \times 10^3$	Exact $U_4 \times 10^3$
(1.10, 0.00)	0.0000	0.0000	0.0000
(0.50, 0.80)	2.6621	2.7870	2.8228
(0.10, 0.70)	6.3796	6.4938	6.5263
(1.90, 0.10)	−1.5416	−1.1523	−1.1403
(0.90, 0.20)	3.2009	3.2672	3.3500
(1.05, 1.05)	−5.2272	−5.0658	−5.0197

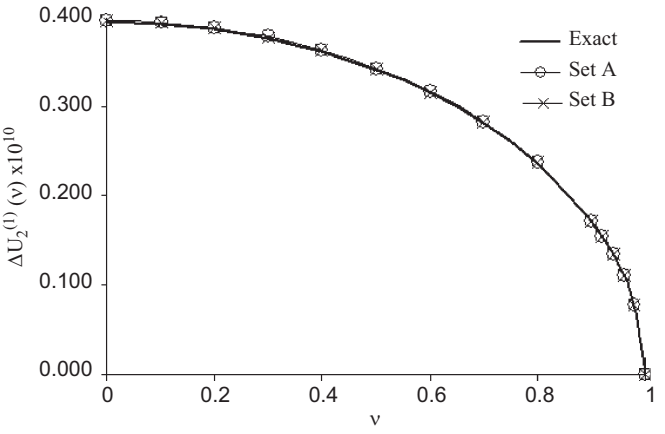

Fig. 2. Plots of $\Delta U_2^{(1)}(\nu) \times 10^{10}$ over $0 \leqslant \nu \leqslant 1$.

those in Set A and show significant convergence towards the exact values.

A graphical comparison between the numerical and the exact crack-opening displacement $\Delta U_2^{(1)}(\nu)$ for the only crack here is given in Fig. 2 for $0 \leqslant \nu \leqslant 1$. Similarly, plots of the numerical and the exact electric potential jump $\Delta U_4^{(1)}(\nu)$ across opposite faces of the crack are given in Fig. 3. The graphs of the numerical $\Delta U_2^{(1)}(\nu)$ and $\Delta U_4^{(1)}(\nu)$ are close to the exact ones. For the particular problem here, note that $\Delta U_2^{(1)}(\nu) = \Delta U_2^{(1)}(-\nu)$ and $\Delta U_4^{(1)}(\nu) = \Delta U_4^{(1)}(-\nu)$ as well as $\Delta U_1^{(1)}(\nu) = 0$ and $\Delta U_3^{(1)}(\nu) = 0$ for $-1 \leqslant \nu \leqslant 1$.

Note that $K_{\mathrm{II}}^{+} = K_{\mathrm{II}}^{-} = 0$ and $K_{\mathrm{III}}^{+} = K_{\mathrm{III}}^{-} = 0$ for the particular problem here. The numerically obtained values of $K_{\mathrm{II}}^{\pm}$ and $K_{\mathrm{III}}^{\pm}$ are not exactly zero but extremely small in magnitude of the order 10^{-15}. A comparison of the numerical and exact values of only $K_{\mathrm{I}}^{\pm}$ and $K_{\mathrm{IV}}^{\pm}$ are given in Table 3. The numerical values are in good agreement with the exact ones, even for Set A in which the discretization of the exterior boundary of the solution domain is relatively crude.

Problem 2. The geometry of the solution domain and the direction of the electrical poling are as in Problem 1. Here the crack is, however, electrically *permeable*.

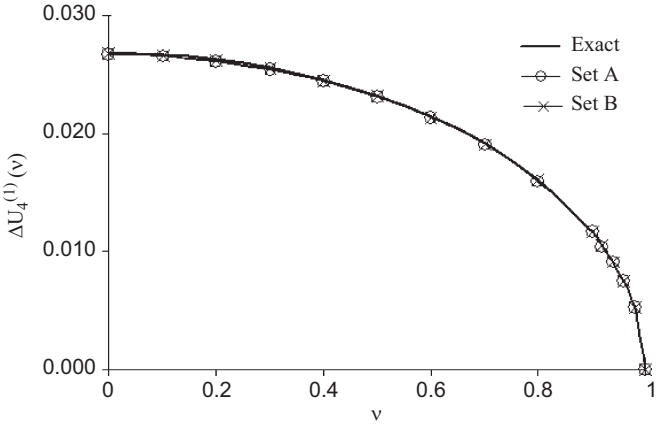

Fig. 3. Plots of $\Delta U_4^{(1)}(\nu)$ over $0 \leqslant \nu \leqslant 1$.

Table 3
Numerical and exact values of the stress and electric displacement intensity factors.

Intensity factor	Set A	Set B	Exact
K_{I}^{+}	1.00400	1.00102	1.00000
K_{I}^{-}	1.00400	1.00102	1.00000
$K_{\mathrm{IV}}^{+} \times 10^{10}$	1.02638	1.00627	1.00000
$K_{\mathrm{IV}}^{-} \times 10^{10}$	1.02638	1.00627	1.00000

Take

$$U_K = \mathrm{Re}\left\{\sum_{\alpha=1}^{4} A_{K\alpha} M_{\alpha 1} (1 + (z_\alpha^2 - a^2)^{1/2})\right\},$$
$$S_{Kj} = \mathrm{Re}\left\{\sum_{\alpha=1}^{4} L_{Kj\alpha} M_{\alpha 1} \frac{z_\alpha}{(z_\alpha^2 - a^2)^{1/2}}\right\}, \tag{54}$$

as a particular electroelastic solution of (9) in the whole of the $0x_1x_2$ plane with a cut in the region $-a < x_1 < a$, $x_2 = 0$.

For the particular values of the constants A, N, F, C, L, e_1, e_2, e_3, ε_1 and ε_2 used in Problem 1, as given in (53), the matrices $[A_{K\alpha}]$ and $[M_{\alpha S}]$ are such that

$$\mathrm{Im}\left\{\sum_{\alpha=1}^{4} A_{4\alpha} M_{\alpha 1}\right\} = 0. \tag{55}$$

Because of (55), the electric potential U_4 given by (54) satisfies

$$\lim_{\varepsilon \to 0^+} [U_4(x_1, \varepsilon) - U_4(x_1, -\varepsilon)] = 0 \quad \text{for} \quad -a < x_1 < a. \tag{56}$$

With the material constants in (53), the functions U_K and S_{Kj} in (54) satisfy the traction-free and electrically permeable conditions ($S_{12} = S_{22} = S_{32} = 0$ and $\Delta U_4^{(1)} = 0$) on the crack $-a < x_1 < a$, $x_2 = 0$. For a particular test problem to check the boundary element procedure and the numerical Green's function for electrically permeable cracks, we use (54) together with (53) to generate boundary values of U_K and P_K on the horizontal and vertical sides of the square domain R, respectively.

To obtain some numerical results, we take $a = 1$ and $h = 2$, divide each side of the square domain into N_0 of equal length and carry out two sets of numerical calculations (Sets A and B as in Problem 1) using the boundary element method. The numerical Green's function for the permeable crack is computed using $J = 10$ in (32). In Tables 4 and 5 numerical values of $U_1 \times 10^{12}$, $U_2 \times 10^{12}$ and U_4 at selected points in the interior of the solution domain are compared with the exact values computed using (54). For the particular problem here, K_{II}^{+} and K_{II}^{-} are the only intensity factors which have non-zero values. Table 6 compares the numerical and

Table 4
Numerical and exact values of $(U_1 \times 10^{12}, U_2 \times 10^{12})$ at selected interior points.

Point (x_1, x_2)	Set A $(U_1, U_2) \times 10^{12}$	Set B $(U_1, U_2) \times 10^{12}$	Exact $(U_1, U_2) \times 10^{12}$
(1.10, 0.00)	(0.00000, −10.926)	(0.0000, −11.068)	(0.0000, −11.111)
(0.50, 0.80)	(32.931, −8.0315)	(32.883, −8.0920)	(32.893, −8.1062)
(0.10, 0.70)	(29.721, −7.5773)	(29.680, −7.5899)	(29.691, −7.5928)
(1.90, 0.10)	(5.7181, −19.721)	(4.3235, −19.796)	(4.3217, −19.899)
(0.90, 0.20)	(13.742, −7.1452)	(13.712, −7.2682)	(13.688, −7.2885)
(1.05, 1.05)	(41.822, −11.510)	(41.739, −11.623)	(41.746, −11.653)

Table 5
Numerical and exact values of U_4 at selected interior points.

Point (x_1, x_2)	Set A $U_4 \times 10^2$	Set B $U_4 \times 10^2$	Exact $U_4 \times 10^2$
(1.10, 0.00)	2.7061	2.7330	2.7425
(0.50, 0.80)	2.8303	2.8399	2.8435
(0.10, 0.70)	2.0639	2.0659	2.0666
(1.90, 0.10)	4.8273	4.9076	4.9262
(090, 0.20)	2.8701	2.8906	2.9028
(1.05, 1.05)	3.8568	3.8776	3.8845

Table 6
Numerical and exact values of the stress intensity factors.

Intensity factor	Set A	Set B	Exact
K_{II}^{+}	1.00155	0.99962	1.00000
K_{II}^{-}	1.00155	0.99962	1.00000

the exact values of K_{II}^{+} and K_{II}^{-}. The numerical values of K_{II}^{+} and K_{II}^{-} are in good agreement with the exact ones for both Sets A and B.

Problem 3. Let us take the solution domain R to be $-h<x_1<h$, $-h<x_2<h$, with three parallel electrically *impermeable* cracks $\gamma^{(1)}$, $\gamma^{(2)}$ and $\gamma^{(3)}$, where h are given positive constants. The crack $\gamma^{(1)}$ lies in the region $-a<x_1<a$, $x_2=0$, $\gamma^{(2)}$ in $-a<x_1<a$, $x_2=d$, and $\gamma^{(3)}$ in $-a<x_1<a$, $x_2=-d$, where a and d are given positive constants (with $a<h$).

The boundary conditions on the exterior boundary of R are given by

$$\left.\begin{aligned} P_1 &= \pm S_0 \\ P_2 &= \pm T_0 \\ P_3 &= 0 \\ P_4 &= \pm D_0 \end{aligned}\right\} \quad \text{for } -h<x_1<h \text{ on } x_2=\pm h,$$

$$\left.\begin{aligned} P_1 &= 0 \\ P_2 &= \pm S_0 \\ P_3 &= 0 \\ P_4 &= 0 \end{aligned}\right\} \quad \text{for } -h<x_2<h \text{ on } x_1=\pm h, \tag{57}$$

where S_0, T_0 and D_0 are given positive constants.

The non-dimensionalized mode I and mode II stress intensity factors and the non-dimensionalized electric displacement intensity factor at the tip $(a,0)$ of the crack $\gamma^{(1)}$ are given by $K_{\mathrm{I}}^{+}/(T_0\sqrt{a})$, $K_{\mathrm{II}}^{+}/(S_0\sqrt{a})$ and $K_{\mathrm{IV}}^{+}/(D_0\sqrt{a})$, respectively. Note that the mode III stress intensity factor is zero here.

Plots of $K_{\mathrm{I}}^{+}/(T_0\sqrt{a})$, $K_{\mathrm{II}}^{+}/(S_0\sqrt{a})$ and $K_{\mathrm{IV}}^{+}/(D_0\sqrt{a})$ against d/a are given in Han and Wang [16] for $h/a\to\infty$ using the material constants

$$\begin{aligned} &A = 12.6\times10^{10}, \quad N = 5.5\times10^{10}, \quad F = 5.3\times10^{10}, \\ &C = 11.7\times10^{10}, \quad L = 3.53\times10^{10}, \\ &e_1 = 17.0, \quad e_2 = -6.5, \quad e_3 = 23.3, \\ &\varepsilon_1 = 151\times10^{-10}, \varepsilon_2 = 130\times10^{-10}, \end{aligned} \tag{58}$$

where the values of A, N, F, C and L are in $\mathrm{N/m^2}$, e_1, e_2 and e_3 are in $\mathrm{C/m^2}$, and ε_1 and ε_2 are in C/(V m). In Han and Wang [16], planar cracks are modeled as continuous distributions of dislocations with density functions to be determined using a numerical procedure.

We employ the boundary element method here to compute $K_{\mathrm{I}}^{+}/(T_0\sqrt{a})$, $K_{\mathrm{II}}^{+}/(S_0\sqrt{a})$ and $K_{\mathrm{IV}}^{+}/(D_0\sqrt{a})$. The exterior boundary of the region R is discretized into 80 boundary elements. To compute the numerical Green's function for the impermeable crack, we use at least $J=10$ in (32). A larger value of J is needed if the non-dimensionalized distance d/a separating the cracks is smaller. For the purpose of comparing the normalized intensity factors here with those in Han and Wang [16], we use the material constants in (58) and take $h/a=30$, $S_0/T_0=1$ and $D_0/T_0=10^{-10}$ C/N. In Fig. 4, we compare plots of the non-dimensionalized intensity factors against d/a with those extracted from Han and Wang [16] for the corresponding case in which $h/a\to\infty$. The two sets of values appear to agree reasonably well with each other.

Problem 4. If the electrical poling is taken to be along the x_3 direction, the constitutive equations are given by

$$\begin{pmatrix} \sigma_{11} \\ \sigma_{22} \\ \sigma_{33} \\ \sigma_{32} \\ \sigma_{31} \\ \sigma_{12} \end{pmatrix} = \begin{pmatrix} A & N & F & 0 & 0 & 0 \\ N & A & F & 0 & 0 & 0 \\ F & F & C & 0 & 0 & 0 \\ 0 & 0 & 0 & L & 0 & 0 \\ 0 & 0 & 0 & 0 & L & 0 \\ 0 & 0 & 0 & 0 & 0 & \frac{1}{2}(A-N) \end{pmatrix} \begin{pmatrix} \gamma_{11} \\ \gamma_{22} \\ \gamma_{33} \\ 2\gamma_{32} \\ 2\gamma_{31} \\ 2\gamma_{12} \end{pmatrix} - \begin{pmatrix} 0 & 0 & e_2 \\ 0 & 0 & e_2 \\ 0 & 0 & e_3 \\ 0 & e_1 & 0 \\ e_1 & 0 & 0 \\ 0 & 0 & 0 \end{pmatrix} \begin{pmatrix} E_1 \\ E_2 \\ E_3 \end{pmatrix} \tag{59}$$

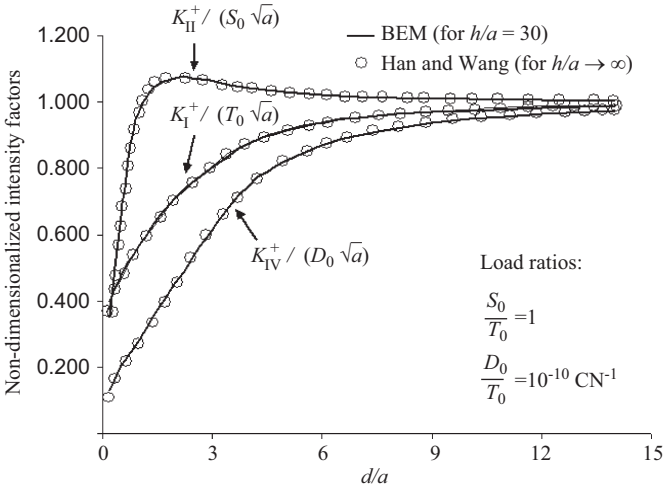

Fig. 4. Plots of $K_{\mathrm{I}}^{+}/(T_0\sqrt{a})$, $K_{\mathrm{II}}^{+}/(S_0\sqrt{a})$ and $K_{\mathrm{IV}}^{+}/(D_0\sqrt{a})$ against d/a.

and

$$\begin{pmatrix} D_1 \\ D_2 \\ D_3 \end{pmatrix} = \begin{pmatrix} 0 & 0 & 0 & 0 & e_1 & 0 \\ 0 & 0 & 0 & e_1 & 0 & 0 \\ e_2 & e_2 & e_3 & 0 & 0 & 0 \end{pmatrix} \begin{pmatrix} \gamma_{11} \\ \gamma_{22} \\ \gamma_{33} \\ 2\gamma_{32} \\ 2\gamma_{31} \\ 2\gamma_{12} \end{pmatrix} + \begin{pmatrix} \varepsilon_1 & 0 & 0 \\ 0 & \varepsilon_1 & 0 \\ 0 & 0 & \varepsilon_2 \end{pmatrix} \begin{pmatrix} E_1 \\ E_2 \\ E_3 \end{pmatrix}. \tag{60}$$

It follows that the non-zero coefficients C_{ijKp} are

$$\begin{aligned} &C_{1111} = C_{2222} = A, \quad C_{1122} = C_{2211} = N, \quad C_{3333} = C, \\ &C_{1133} = C_{3311} = C_{2233} = C_{3322} = F, \\ &C_{1313} = C_{3113} = C_{3131} = C_{1331} = C_{2323} = C_{3223} = C_{3232} = C_{2332} = L, \\ &C_{1212} = C_{2112} = C_{2121} = C_{1221} = \tfrac{1}{2}(A-N), \\ &C_{3141} = C_{1341} = C_{2342} = C_{3242} = C_{4131} = C_{4113} = C_{4223} = C_{4232} = e_1, \\ &C_{1143} = C_{2243} = C_{4311} = C_{4322} = e_2, \\ &C_{3343} = C_{4333} = e_3, \quad C_{4141} = C_{4242} = -\varepsilon_1, \quad C_{4343} = -\varepsilon_2. \end{aligned} \tag{61}$$

The homogeneous system of linear algebraic equations for working out $A_{K\alpha}$ is given by

$$\begin{pmatrix} A+\frac{1}{2}(A-N)\tau_\alpha^2 & (N+\frac{1}{2}(A-N))\tau_\alpha & 0 & 0 \\ (N+\frac{1}{2}(A-N))\tau_\alpha & \frac{1}{2}(A-N)+A\tau_\alpha^2 & 0 & 0 \\ 0 & 0 & L+L\tau_\alpha^2 & e_1+e_1\tau_\alpha^2 \\ 0 & 0 & e_1+e_1\tau_\alpha^2 & -\varepsilon_1-\varepsilon_1\tau_\alpha^2 \end{pmatrix} \times \begin{pmatrix} A_{1\alpha} \\ A_{2\alpha} \\ A_{3\alpha} \\ A_{4\alpha} \end{pmatrix} = \begin{pmatrix} 0 \\ 0 \\ 0 \\ 0 \end{pmatrix}. \tag{62}$$

If we use (62), we find that we cannot construct $[A_{K\alpha}]$ that is invertible. To overcome this minor difficulty, a relatively small amount of anisotropy is introduced into the equations governing u_1 and u_2. Specifically, we replace $C_{1111} = A$ in (61) by $C_{1111} = A + \varepsilon$, where ε is a selected real number whose magnitude is very small compared to A. It follows that we supercede (62) by

$$\begin{pmatrix} A+\varepsilon+\frac{1}{2}(A-N)\tau_\alpha^2 & (N+\frac{1}{2}(A-N))\tau_\alpha & 0 & 0 \\ (N+\frac{1}{2}(A-N))\tau_\alpha & \frac{1}{2}(A-N)+A\tau_\alpha^2 & 0 & 0 \\ 0 & 0 & L+L\tau_\alpha^2 & e_1+e_1\tau_\alpha^2 \\ 0 & 0 & e_1+e_1\tau_\alpha^2 & -\varepsilon_1-\varepsilon_1\tau_\alpha^2 \end{pmatrix} \times \begin{pmatrix} A_{1\alpha} \\ A_{2\alpha} \\ A_{3\alpha} \\ A_{4\alpha} \end{pmatrix} = \begin{pmatrix} 0 \\ 0 \\ 0 \\ 0 \end{pmatrix}. \tag{63}$$

We can take $\tau_3 = \tau_4 = i$ and τ_1 and τ_2 are two distinct solutions with positive imaginary parts of the quartic equation

$$\det \begin{pmatrix} A+\varepsilon+\frac{1}{2}(A-N)\tau^2 & (N+\frac{1}{2}(A-N))\tau \\ (N+\frac{1}{2}(A-N))\tau & \frac{1}{2}(A-N)+A\tau^2 \end{pmatrix} = 0. \tag{64}$$

Note that (64) cannot yield two distinct solutions with positive imaginary parts if ε is zero.

From (62), we find that $A_{K\alpha}$ may be chosen to be

$$\begin{aligned} &A_{1\alpha} = -\frac{(N+\frac{1}{2}(A-N))\tau_\alpha}{A+\varepsilon+\frac{1}{2}(A-N)\tau_\alpha^2}(\delta_{\alpha 1}+\delta_{\alpha 2}), \\ &A_{2\alpha} = \delta_{\alpha 1}+\delta_{\alpha 2}, \quad A_{3\alpha} = \delta_{\alpha 3}, \quad A_{4\alpha} = \delta_{\alpha 4}. \end{aligned} \tag{65}$$

The matrix $[A_{K\alpha}]$ as constructed in (65) is invertible if $\tau_1 \neq \tau_2$.

For a particular problem in which the electrical poling is along the x_3 direction, let us take the solution domain R to be $-h<x_1<h$, $-h<x_2<h$, with two collinear *permeable* crack lying in the regions $-b<x_1<-a$, $x_2=0$, and $a<x_1<b$, $x_2=0$,where a, b and h are positive constants such that $a<b<h$. The boundary conditions on the exterior boundary of R are given by

$$\left.\begin{aligned} P_1 &= 0 \\ P_2 &= 0 \\ P_3 &= \pm S_0 \\ P_4 &= \pm D_0 \end{aligned}\right\} \quad \text{for } -h<x_1<h \text{ on } x_2 = \pm h,$$

$$\left.\begin{aligned} P_1 &= 0 \\ P_2 &= 0 \\ P_3 &= 0 \\ P_4 &= 0 \end{aligned}\right\} \quad \text{for } -h<x_2<h \text{ on } x_1 = \pm h, \tag{66}$$

where S_0 and D_0 are non-negative constants.

Let $K_{\mathrm{III}}^{\mathrm{inner}}$ and $K_{\mathrm{III}}^{\mathrm{outer}}$, respectively, denote the mode III stress intensity factor at the inner and outer tips of the collinear cracks. The crack energy release rates at the inner and outer tips are then, respectively, given by

$$G^{\mathrm{inner}} = \frac{\pi}{2L}(K_{\mathrm{III}}^{\mathrm{inner}})^2 \quad \text{and} \quad G^{\mathrm{outer}} = \frac{\pi}{2L}(K_{\mathrm{III}}^{\mathrm{outer}})^2. \tag{67}$$

In Li [18], it is analytically given that

$$\left(\frac{4LG^{\mathrm{inner}}}{\pi(b-a)S_0^2}, \frac{4LG^{\mathrm{outer}}}{\pi(b-a)S_0^2}\right) \to \left(\frac{2[b^2\lambda - a^2]^2}{a(b-a)(b^2-a^2)}, \frac{2b^3[1-\lambda]^2}{(b-a)(b^2-a^2)}\right) \quad \text{as } 2h/(b-a) \to \infty, \tag{68}$$

where

$$\lambda = \frac{\int_0^{\pi/2}[1-(1-(a/b)^2)\sin^2 t]^{1/2}\,dt}{\int_0^{\pi/2}[1-(1-(a/b)^2)\sin^2 t]^{-1/2}\,dt}. \tag{69}$$

Using the material constants in (58) and taking $2h/(b-a) = 20$, we use the boundary element method with Green's function for the permeable cracks to compute the crack energy release rates G^{inner} and G^{outer} according to (67) (after calculating numerically the mode III stress intensity factors). In perturbing the elastic modulus C_{1111} to construct an invertible matrix $[A_{K\alpha}]$, we choose $\varepsilon = 10^2$, that is, we take C_{1111} to be given by $(12.6 + 10^{-8}) \times 10^{10}$ N/m^2 instead of 12.6×10^8 N/m^2. The outer boundary of the solution domain is discretized into 160 elements. The numerical Green's function is calculated using at least $J = 10$ in (32). If the inner tips of the cracks are close to each other then $J = 30$ is used. If the outer tips are near the vertical sides, we use $J = 20$ and add another 40 elements on each of the vertical sides.

Plots of the non-dimensionalized crack energy release rates $4LG^{\mathrm{inner}}/(\pi(b-a)S_0^2)$ and $4LG^{\mathrm{outer}}/(\pi(b-a)S_0^2)$ against $2a/(b-a)$ (for $0.50 \leqslant 2a/(b-a) \leqslant 17.50$) are given in Figs. 5 and 6, respectively. In the figures, we also compare the numerical crack energy release rates with the values calculated from (68) (given by Li [18] for $2h/(b-a) \to \infty$). The numerical crack energy release rates are found to agree very well with (68) for small values of $2a/(b-a)$. This is expected as (68) is valid only for $2h/(b-a) \to \infty$ (that is, for an infinite piezoelectric material).

Note that the crack tip energy release rate G for the corresponding problem involving only a single crack of length

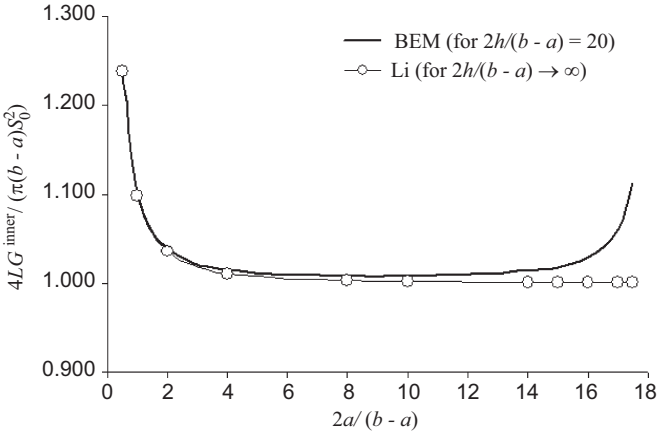

Fig. 5. Plots of $4LG_{\mathrm{I}}^{\mathrm{inner}}/(\pi(b-a)S_0^2)$, against $2a/(b-a)$.

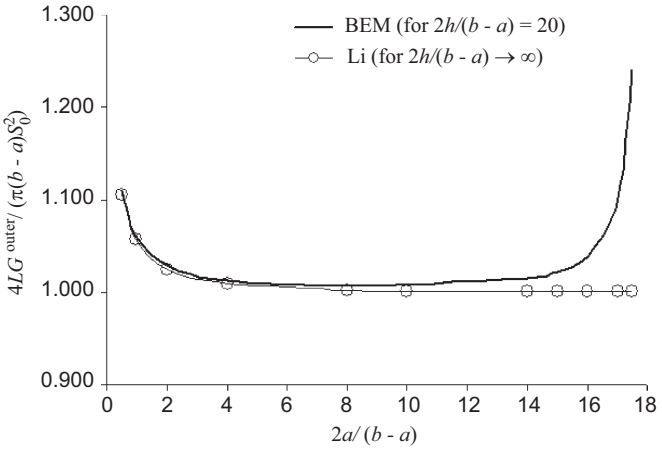

Fig. 6. Plots of $4LG_{\mathrm{I}}^{\mathrm{outer}}/(\pi(b-a)S_0^2)$, against $2a/(b-a)$.

$b-a$ in an infinite piezoelectric material is given by $4LG/(\pi(b-a)S_0^2)=1$. Thus, it is not surprising that $4LG^{\mathrm{inner}}/(\pi(b-a)S_0^2)$ and $4LG^{\mathrm{outer}}/(\pi(b-a)S_0^2)$ computed using the boundary element method are quite close to 1 when the inner crack tips are several crack lengths apart and the outer tips are not yet so close to the vertical sides of the solution domain. As $2a/(b-a)$ approaches 18 (that is, as the outer crack tips approach the vertical sides of the solution domain), the crack energy release rates calculated using the boundary element method begin to deviate more significantly from (68). As expected, as is obvious in Fig. 6, $4LG^{\mathrm{outer}}/(\pi(b-a)S_0^2)$ shows a significant increase in magnitude when the outer crack tips interact strongly with the vertical sides of the solution domain.

For the particular problem under consideration here, it is known theoretically that $4LG^{\mathrm{inner}}/(\pi(b-a)S_0^2)$ for $2a/(b-a)=\xi$ (where ξ is a positive real number such that $0<\xi<18$) is equal to $4LG^{\mathrm{outer}}/(\pi(b-a)S_0^2)$ for $2a/(b-a)=18-\xi$. Also, $4LG^{\mathrm{outer}}/(\pi(b-a)S_0^2)$ for $2a/(b-a)=\xi$ is equal to $4LG^{\mathrm{inner}}/(\pi(b-a)S_0^2)$ for $2b/(b-a)=18-\xi$. In Figs. 5 and 6, the graphs for the numerical values of $4LG^{\mathrm{inner}}/(\pi(b-a)S_0^2)$ and $4LG^{\mathrm{outer}}/(\pi(b-a)S_0^2)$ as obtained from the boundary element method reflect this theoretical observation. For example, we find that the values of $4LG^{\mathrm{inner}}/(\pi(b-a)S_0^2)$ for $2a/(b-a)=0.50$ and $4LG^{\mathrm{outer}}/(\pi(b-a)S_0^2)$ for $2a/(b-a)=17.50$ are, respectively, given by 1.2425 and 1.2407 (which differ from each other by less than 0.2%), and $4LG^{\mathrm{outer}}/(\pi(b-a)S_0^2)$ for $2a/(b-a)=0.50$ and $4LG^{\mathrm{inner}}/(\pi(b-a)S_0^2)$ for $2a/(b-a)=17.50$ are, respectively, given by 1.1024 and 1.1021 (less than 0.03% difference).

7. Summary

Green's functions are constructed numerically for multiple arbitrarily located planar cracks in an infinite electroelastic space. The cracks are traction free and electrically either permeable or impermeable. We apply the Green's functions to derive a simple boundary element method for the numerical solution of some plane electroelastic crack problems involving finite solution domains. As the Green's functions satisfy the boundary conditions on the cracks, the boundary element procedure requires only the exterior boundary of the solution domain to be discretized into boundary elements, that is, no discretization of the crack faces is needed.

To check the validity of the numerical Green's functions and the boundary element method, some specific electroelastic crack problems are solved. Numerical values obtained for the relevant intensity factors and the crack energy release rate at the crack tips are in good agreement with the values computed from known solutions in the literature.

References

[1] Abramowitz M, Stegun IA. Handbook of mathematical functions. New York: Dover; 1971.
[2] Ang WT. A boundary integral solution for the problem of multiple interacting cracks in an elastic material. International Journal of Fracture 1986;31:259–70.
[3] Ang WT. A boundary integral equation for deformations of an elastic body with an arc crack. Quarterly of Applied Mathematics 1987;45:131–9.
[4] Ang WT, Clements DL. A boundary integral equation method for the solution of a class of crack problems. Journal of Elasticity 1987;17:9–21.
[5] Ang WT, Park YS. Hypersingular integral equations for arbitrarily-located planar cracks in an anisotropic bimaterial. Engineering Analysis with Boundary Elements 1997;20:135–43.
[6] Ang WT, Telles JCF. A numerical Green's function for multiple cracks in anisotropic bodies. Journal of Engineering Mathematics 2004;49:197–207.
[7] Barnett DM, Lothe J. Dislocations and line charges in anisotropic piezoelectric insulators. Physica Status Solidi (b) 1975;67:105–11.
[8] Chen JT, Hong HK. Review of dual boundary element methods with emphasis on hypersingular integrals and divergent series. Applied Mechanics Review 1999;52:17–33.
[9] Clements DL. Boundary value problems governed by second order elliptic systems. London: Pitman; 1981.
[10] Clements DL, Haselgrove MD. A boundary integral equation method for a class of crack problems in anisotropic elasticity. International Journal of Computer Mathematics 1983;12:267–78.
[11] Ding HJ, Wang GQ, Chen WQ. A boundary integral formulation and 2D fundamental solutions for piezoelectric media. Computer Methods in Applied Mechanics and Engineering 1998;158:65–80.
[12] Gao GF, Fan WX. The fundamental solutions for the plane problem in piezoelectric media with an elliptic hole or a crack. Applied Mathematics and Mechanics 1998;19:1043–52.
[13] Garcia-Sanchez F, Saez SB, Dominguez J. Anisotropic and piezoelectric materials fracture analysis by BEM. Computers & Structures 2005;83:804–20.
[14] Groh U, Kuna M. Efficient boundary element analysis of cracks in 2D piezoelectric structures. International Journal of Solids and Structures 2005;42:2399–416.
[15] Guimarães S, Telles JCF. General application of numerical Green's functions for SIF computations with boundary elements. Computer Modeling in Engineering and Sciences 2000;1:131–9.
[16] Han X, Wang T. Interacting multiple cracks in piezoelectric materials. International Journal of Solids and Structures 1999;36:4183–202.
[17] Kaya AC, Erdogan F. On the solution of integral equations with strongly singular kernels. Quarterly of Applied Mathematics 1987;45:105–22.
[18] Li XF. Closed-form solution for a piezoelectric strip with two collinear cracks normal to the strip boundaries. European Journal of Mechanics-A/Solids 2002;21:981–9.
[19] Park SB, Sun CT. Fracture criteria for piezoelectric ceramics. Journal of the American Ceramic Society 1995;78:1475–80.
[20] Rajapakse RKND, Xu XL. Boundary element modeling of cracks in piezoelectric solids. Engineering Analysis with Boundary Elements 2001;25:771–81.

[21] Shindo Y, Tanaka K, Narita F. Singular stress and electric fields of a piezoelectric ceramic strip with a finite crack under longitudinal stress. Acta Mechanica 1997;120:31–45.
[22] Snyder MD, Cruse TA. Boundary integral analysis of cracked anisotropic plates. International Journal of Fracture 1975;11:315–28.
[23] Telles JCF, Castor GS, Guimarães S. A numerical Green's function approach for boundary elements applied to fracture mechanics. International Journal for Numerical Methods in Engineering 1995;38:3259–74.
[24] Wang BL, Mai YW. Impermeable crack and permeable crack assumptions, which one is more realistic? Journal of Applied Mechanics—Transactions of ASME 2004;71:575–8.
[25] Xu XL, Rajapakse RKND. Boundary element analysis of piezoelectric solids with defects. Composites Part B: Engineering 1998;29:655–69.